

Solution of the antiferromagnetic Ising model with multisite interaction on a zigzag ladder

E. Jurčišinová and M. Jurčišin

Institute of Experimental Physics, Slovak Academy of Sciences, Watsonova 47, 040 01 Košice, Slovakia

(Received 9 April 2014; published 9 September 2014)

We consider the antiferromagnetic spin-1/2 Ising model with multisite interaction in an external magnetic field on an infinite zigzag ladder. The model is solved exactly by using the transfer matrix method. Using the exact expression for the total magnetization per site, the magnetic properties of the model are investigated in detail. The model exhibits the formation of magnetization plateaus for low temperatures, and it is shown that their properties depend strongly on the strength of the multisite interaction. All possible ground states of the model are found and discussed. The existence of nontrivial singular ground states is proven and exact explicit expressions for them are found. The macroscopic degeneracy of the ground states is investigated and discussed.

DOI: [10.1103/PhysRevE.90.032108](https://doi.org/10.1103/PhysRevE.90.032108)

PACS number(s): 05.50.+q, 75.10.Hk, 75.50.Ee

I. INTRODUCTION

One of the most interesting phenomena from the experimental as well as the theoretical point of view observed in the framework of antiferromagnetic systems on various lattices is without doubt the phenomenon of frustration (see, e.g., Ref. [1] and references cited therein). Roughly speaking, an antiferromagnetic model on a regular lattice is fully frustrated if all elementary (minimal) closed contours are formed by odd number of sites [2]. Among the most interesting frustrated models from the phenomenological point of view are antiferromagnetic models on the kagome lattice, on the triangular lattice, and on the tetrahedron (pyrochlore) lattice. While the first two of them represent examples of two-dimensional geometrically frustrated systems the third one is an example of a three-dimensional frustrated system. Although, for a deeper theoretical understanding of basic properties of various frustrated systems, exact solutions of the corresponding models are the most valuable, nowadays only very few such frustrated models in two dimensions have been exactly solved (for a review see, e.g., Refs. [3,4]). It is also worth mentioning that even the simplest Ising and Ising-like models on regular two-dimensional lattices have been exactly solved only in zero external magnetic field (see, e.g., Ref. [5] and references cited therein). In this respect, e.g., the exact solution of the antiferromagnetic Ising model in zero external magnetic field on a triangular lattice has been known for a long time [6]. However, it is also well known that the most interesting physical effects related to frustration appear when an external magnetic field is present (e.g., the formation of magnetization plateaus when the temperature tends to zero). In this situation, it is evident that to obtain relevant theoretical information about properties of various frustrated systems in an external magnetic field it is necessary to use an approximation.

An elegant technique for approximative investigation of frustrated effects on real lattices is based on the analysis of antiferromagnetic models on various recursive lattices, which, on one hand, take into account the basic geometric structure of real lattices that is responsible for frustration and, on the other hand, are exactly solvable. Quite recently exact solutions were obtained for antiferromagnetic spin-1/2 Ising models on the corresponding pure Husimi lattice, which represents an effective approximation of the model on the kagome lattice

[7,8] as well as on the tetrahedron recursive lattice [9]. The existence of these solutions has allowed authors to perform complete analyses of all possible ground states of the models. Maybe the most intriguing result of these investigations is the fact of the existence of so-called singular ground states, i.e., ground states which are realized only for exactly defined values of the external magnetic field for fixed values of all the other parameters of the model, with exactly defined values of the magnetization. Thus, it seems that transition between various magnetization plateaus (the long-range-order ground states) is always realized only through nontrivial singular ground states (see discussions in Refs. [7–9]). However, here a legitimate question immediately arises, namely, whether the existence of the singular ground states is related only to the recursive nature of the lattices or whether the singular ground states are also always present in classical antiferromagnetic models on regular geometrically frustrated lattices. It is evident that to answer this question it is necessary to solve exactly at least one classical antiferromagnetic model on a regular lattice. In the present paper, we shall show that such an exactly solvable antiferromagnetic model on a regular lattice really exists, namely, we shall find the exact solution of the antiferromagnetic spin-1/2 Ising model in the simultaneous presence of multisite interaction and an external magnetic field on the so-called zigzag ladder. We shall perform a detailed exact analysis of the magnetization properties of the model and we shall see that the model exhibits rather interesting behavior with a nontrivial structure of the ground states which consists of long-range-order ground states as well as of the above-mentioned singular ground states which are realized on the borders of the magnetization plateaus. Although the model is an example of an antiferromagnetic model on a regular one-dimensional lattice (or on a quasi-two-dimensional lattice), nevertheless we think that the results obtained (at least at the qualitative level) have to be considered seriously and that similar properties of the magnetization as well as of the ground states as functions of the external magnetic field should also be expected on regular geometrically frustrated two- and three-dimensional lattices in accordance with (again at least at the qualitative level) the results obtained earlier in the framework of antiferromagnetic models on recursive lattices (see Refs. [7–9]).

Finally, let us note that various antiferromagnetic models on ladderlike lattices are also phenomenologically significant and

are used for theoretical investigations of various physical systems such as SrCuO₂ [10,11], SrCu₂O₃ [12], La₆Ca₈Cu₂₄O₄₁ [13,14], Cu₂(C₅H₁₂N₂)₂Cl₄ [15], KCuCl₃ and TiCuCl₃ [16], NH₄CuCl₃ [17], Li₂CuO₂ and CuGeO₃ [14], NaCu₂O₂ [18], and many others. Although for theoretical investigation of these systems various variants of the quantum Heisenberg model are usually used (see, e.g., Refs. [19–30] and references cited therein), nevertheless some properties of these systems, such as the very formation of magnetization plateaus at low temperatures (which have in fact a quantum nature), can also be studied in the framework of the corresponding classical models, e.g., in the framework of antiferromagnetic Ising and Ising-like models (see, e.g., Refs. [31–34] and references cited therein). Here, the main advantage of the classical models in comparison to the quantum ones is the fact that very often they can be solved exactly, i.e., many interesting properties of the corresponding systems can be studied and analyzed in a completely exact way (e.g., the exact structure of the ground states as shown in the present paper). Therefore, we believe that the exact results obtained in the present paper can be considered as an interesting and important contribution for deeper understanding of the magnetic properties of various classical frustrated systems even in cases when the exact solutions do not exist yet.

The paper is organized as follows. In Sec. II, the antiferromagnetic Ising model with multisite interaction on the zigzag ladder is defined. In Sec. III, the exact solution of the model is presented by using the transfer matrix method. In Sec. IV, the properties of the magnetization are studied, and all ground states of the model are found and their properties are discussed. In Sec. V, the main results of the paper are reviewed.

II. THE ANTIFERROMAGNETIC ISING MODEL WITH MULTISITE INTERACTION ON THE ZIGZAG LADDER

In what follows, we shall study the magnetic properties of the antiferromagnetic spin-1/2 Ising model with multisite interaction within elementary triangles in an external magnetic field on the infinite zigzag ladder shown in Fig. 1. Thus, each site has the coordination number $z = 4$ and the Hamiltonian of the model is

$$\mathcal{H} = -J \sum_{\langle i j \rangle} s_i s_j - J' \sum_{\langle i j k \rangle} s_i s_j s_k - H \sum_i s_i, \quad (1)$$

where each variable s_i acquires one of the two possible values ± 1 , J is the nearest-neighbor interaction parameter, J' represents the multisite interaction within single triangles, and H is the external magnetic field. In Eq. (1), the first sum runs over all nearest-neighbor spin pairs, the second sum runs over all triangles, and the third sum runs over all spin sites. In

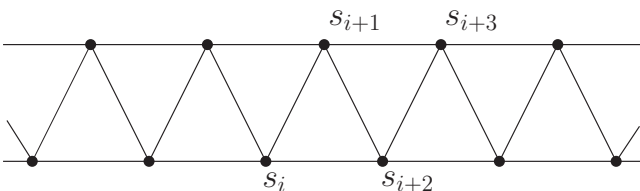


FIG. 1. The structure of the infinite triangular zigzag ladder.

what follows, we are interested only in the antiferromagnetic system, i.e., we always suppose that $J < 0$.

The partition function of the model given by the Hamiltonian (1) has the following general form:

$$\begin{aligned} Z &\equiv \sum_s e^{-\beta \mathcal{H}} \\ &= \sum_s e^{K \sum_{\langle i j \rangle} s_i s_j + K' \sum_{\langle i j k \rangle} s_i s_j s_k + h \sum_i s_i}, \end{aligned} \quad (2)$$

where the standard notation is used, namely, $\beta = 1/(k_B T)$, T is the temperature, k_B is the Boltzmann constant, $K = \beta J$, $K' = \beta J'$, and $h = \beta H$. The sum over s in Eq. (2) means the summation over all possible spin configurations on the lattice.

III. EXACT SOLUTION OF THE MODEL BY THE TRANSFER MATRIX METHOD

As was already mentioned, our aim is to investigate model (1) on the infinite zigzag ladder. For this purpose it is convenient to introduce cyclic conditions (periodic boundary conditions), i.e., we start with the assumption that the number of all sites is finite and equal to N , where N is even, and we suppose that $s_{N+1} = s_1$ or, in general, $s_{N+i} = s_i$. Introducing cyclic conditions ensures that all sites are equivalent as well as that the system obeys translational symmetry. Then, the infinite zigzag ladder is obtained in the limit $N \rightarrow \infty$.

Using the periodic boundary conditions the partition function (2) for the present model can be written in the standard transfer matrix form

$$Z = \text{Tr} V^{N/2}, \quad (3)$$

where V is the square transfer matrix which has the following explicit form:

$$V = \begin{pmatrix} a^4 b c^2 & a c & (a b)^{-1} c & a^{-2} \\ (a b)^{-1} c & 1 & a^{-2} b & a c^{-1} \\ a c & a^{-2} b^{-1} & 1 & b (a c)^{-1} \\ a^{-2} & b (a c)^{-1} & a c^{-1} & a^4 b^{-1} c^{-2} \end{pmatrix}, \quad (4)$$

where

$$a = e^K, \quad b = e^{2K'}, \quad c = e^h. \quad (5)$$

It also means that the partition function can be written in the form of the sum of the $(N/2)$ th power of the eigenvalues of the transfer matrix (4), namely,

$$Z_N = \sum_{i=1}^4 \lambda_i^{N/2}, \quad (6)$$

where λ_i , $i = 1, \dots, 4$, represent the eigenvalues of the transfer matrix.

Because the characteristic equation of the transfer matrix (4) is a polynomial equation of the fourth order, the transfer matrix can have four real eigenvalues, two real eigenvalues together with two complex conjugate eigenvalues, or even two pairs of complex conjugate eigenvalues. However, by direct numerical analysis of the eigenvalues it can be shown that the transfer matrix (4) always has at least two real eigenvalues. At the same time, one real eigenvalue is always larger than the other three real eigenvalues (in the case when all eigenvalues

are real) or it is also larger than the second real eigenvalue as well as than the absolute values of the two remaining complex conjugate eigenvalues. Thus, let λ_1 be the largest eigenvalue. Then, writing Eq. (6) in the form

$$Z_N = \lambda_1^{N/2} \left[1 + \sum_{i=2}^4 \left(\frac{\lambda_i}{\lambda_1} \right)^{N/2} \right], \quad (7)$$

it is evident that in the limit $N \rightarrow \infty$ the partition function is completely determined by the eigenvalue λ_1 itself, namely,

$$Z_N = \lambda_1^{N/2}, \quad N \rightarrow \infty. \quad (8)$$

However, for further analysis more important is the free energy per site defined in the standard way by the partition function as follows:

$$f = -(\beta N)^{-1} \ln Z_N, \quad (9)$$

which in the limit $N \rightarrow \infty$ [by using Eq. (8)] obtains the simple form

$$f = -\frac{\ln \lambda_1}{2\beta}. \quad (10)$$

Thus, from Eqs. (8) and (10) it follows that all properties of the model on the infinite zigzag ladder are given by a single quantity, namely, by the largest eigenvalue λ_1 of the transfer matrix. Therefore, if an explicit analytic expression for λ_1 exists then the model belongs among exactly solvable models. The explicit expression for λ_1 really exists and has the form

$$\lambda_1 = \frac{1}{4} \left[k_1 + 2\sqrt{z_1 + w_1} + \sqrt{4(2z_1 - w_1) + \frac{z_2}{\sqrt{z_1 + w_1}}} \right], \quad (11)$$

where

$$k_1 = 2 + a^4 \left(bc^2 + \frac{1}{bc^2} \right), \quad (12)$$

$$w_1 = \frac{1}{3} \left[\left(\frac{w_2}{2} \right)^{1/3} + z_3 \left(\frac{2}{w_2} \right)^{1/3} \right], \quad (13)$$

$$z_1 = \frac{k_1^2}{4} - \frac{2k_4}{3}, \quad (14)$$

$$z_2 = k_1^3 - 4k_1k_4 - 8k_3, \quad (15)$$

and

$$w_2 = z_4 + \sqrt{z_4^2 - 4z_3^3}, \quad (16)$$

$$z_3 = k_4^2 + 12k_2 + 3k_1k_3, \quad (17)$$

$$z_4 = 2k_4^3 + 9 \left[3(k_1^2k_2 + k_3^2) + k_4(k_1k_3 - 8k_2) \right], \quad (18)$$

$$k_2 = [b^2(1 + a^8) - a^4(1 + b^4)]^2 / (a^8b^4), \quad (19)$$

$$k_3 = -\{b^2(b^2 - a^4)^2 + 2a^4bc^2[b^2(1 + a^8) - a^4(1 + b^4)] + c^4(a^4b^2 - 1)^2\} / (a^4b^3c^2), \quad (20)$$

$$k_4 = \{2a^4[a^4 - b^2 + c^4(a^4b^2 - 1)] + bc^2(a^{12} + a^4 - 2)\} / (a^4bc^2), \quad (21)$$

and a , b , and c are defined in Eq. (5).

Therefore, having the exact analytic expression for the largest eigenvalue λ_1 as it is given in Eqs. (11)–(21) one can immediately use it for investigation of all important quantities such as the magnetization, susceptibility, or specific heat, which are defined as the corresponding derivatives of the free energy (10). However, in what follows we shall concentrate only on the magnetic properties of the model. Our aim is to investigate in detail the frustration effects for low enough temperatures as well as to find the full structure of the ground states of the model.

Finally, it is also worth mentioning that the exact analytic solution of the present model also exists on the zigzag lattice with periodic boundary conditions with arbitrary finite number of sites N (recall once more that N must be even). However, here all four eigenvalues of the transfer matrix (4) must be taken into account (it can be shown that analytic expressions also exist for all three remaining eigenvalues) and, of course, in this case all results strongly depend on the value of N , especially for low enough values of N .

IV. MAGNETIZATION AND THE GROUND STATES OF THE MODEL

A. Magnetization properties of the model

The magnetization per site is given by the relation

$$m \equiv -\frac{\partial f}{\partial H} = -\beta \frac{\partial f}{\partial h}, \quad (22)$$

taken at a constant temperature. Now, using Eq. (10) the magnetization per site is given directly by the eigenvalue λ_1 , namely,

$$m = \frac{1}{2\lambda_1} \frac{\partial \lambda_1}{\partial h}. \quad (23)$$

Having at hand the explicit expression for the largest eigenvalue λ_1 as it is given in Eqs. (11)–(21) one can also easily write out the corresponding explicit expression for the magnetization. Therefore, it is not necessary to present its explicit form here.

The typical behavior of the total magnetization as a function of the external magnetic field for various values of the ratio $\alpha = J'/|J|$ and for various values of the reduced temperature $k_B T/|J|$ is shown in Figs. 2–8. As it is evident from Fig. 2, in the case when the multisite interaction is not present in the model ($\alpha = 0$) the magnetization exhibits the formation of three magnetization plateaus (the long-range-order ground states) when the temperature tends to zero with the values of magnetization $m = 0$ and $m = \pm 1/3$. Each of them appears in the corresponding interval of the external magnetic field, namely, the magnetization plateau with $m = 0$ is realized in the interval $-1 < H/|J| < 1$ and the magnetization plateaus with $m = 1/3$ and $m = -1/3$ are realized in the intervals $1 < H/|J| < 4$ and $-4 < H/|J| < -1$, respectively.

On the other hand, when multisite interaction is present in the model the behavior of the total magnetization as well as the structure and the length of the plateaus are significantly changed. As we shall see, there exist three disjoint intervals of the absolute values of α in which qualitatively different behavior of the total magnetization is observed. First of all, in the interval $-0.5 < \alpha < 0.5$, i.e., for $|\alpha| < 0.5$, the behavior

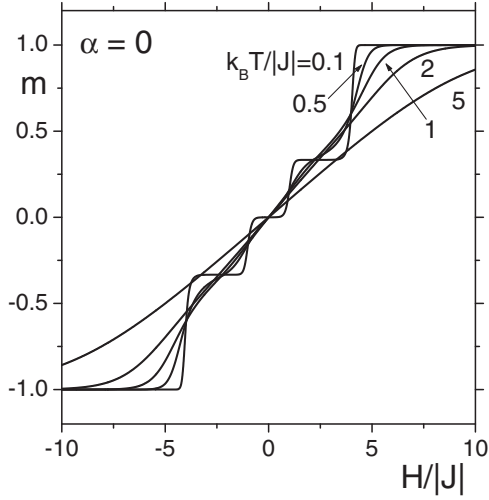


FIG. 2. The total magnetization per site as a function of the external magnetic field for $\alpha = 0$ and for various values of the reduced temperature.

of the total magnetization for low temperatures is qualitatively similar to the case with $\alpha = 0$, i.e., there still emerge three magnetization plateaus with $m = 0$ and $m = \pm 1/3$ when the temperature tends to zero, but now they are realized in intervals of the external magnetic field boundaries which depend on the value of α . Namely, the magnetization plateau with $m = 0$ is realized in the interval $-1 + 3\alpha < H/|J| < 1 + 3\alpha$, the magnetization plateau with $m = -1/3$ is realized in the interval $-4 - 3\alpha < H/|J| < -1 + 3\alpha$, and, finally, the plateau with $m = 1/3$ exists in the interval $1 + 3\alpha < H/|J| < 4 - 3\alpha$. Thus, it is evident that while the length of the plateau with $m = 0$ is not changed in this interval of values of α the lengths of the magnetization plateaus with $m = \pm 1/3$ significantly depend not only on the absolute value of α but also on its sign. Here, for $-0.5 < \alpha < 0$, the length of the plateau with $m = 1/3$ increases when the absolute value of α increases. At the same time, the length of the plateau with $m = -1/3$

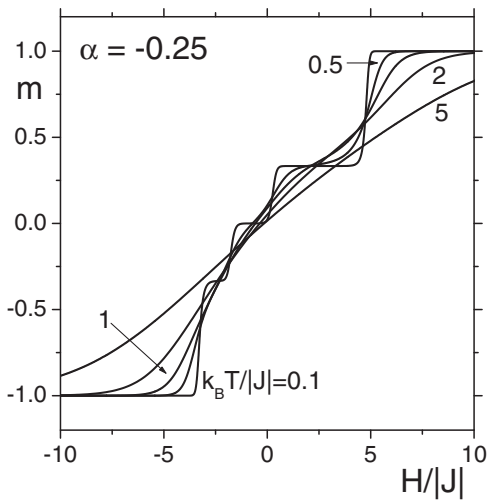


FIG. 3. The total magnetization per site as a function of the external magnetic field for $\alpha = -0.25$ and for various values of the reduced temperature.

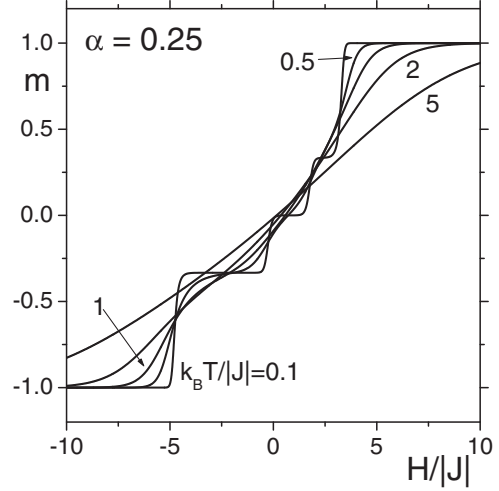


FIG. 4. The total magnetization per site as a function of the external magnetic field for $\alpha = 0.25$ and for various values of the reduced temperature.

decreases and completely vanishes when α tends to -0.5 . On the other hand, the situation in the interval $0 < \alpha < 0.5$ is opposite. Here, the length of the magnetization plateau with $m = -1/3$ increases when α is increasing and the length of the plateau with $m = 1/3$ decreases and vanishes completely for $\alpha = 0.5$. The typical behavior of the total magnetization as a function of the external magnetic field for positive as well as negative values of α from the interval $-0.5 < \alpha < 0.5$ for various values of the temperature is shown in Figs. 3 and 4 for $\alpha = -0.25$ and $\alpha = 0.25$, respectively.

The second qualitatively different type of behavior of the magnetization is realized in the interval $0.5 < |\alpha| < 1$ as it is evident in Figs. 5 and 6, where the total magnetization as a function of the external magnetic field for various values of the temperature is shown for $\alpha = -0.75$ (Fig. 5) and $\alpha = 0.75$ (Fig. 6). In this interval of the absolute values of α only two magnetization plateaus appear when the temperature tends to zero and, at the same time, their lengths also depend on the

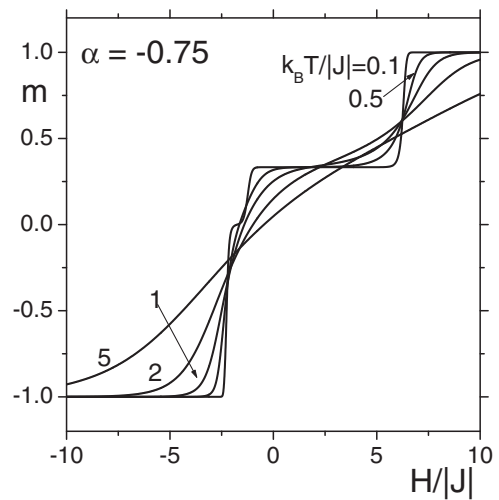


FIG. 5. The total magnetization per site as a function of the external magnetic field for $\alpha = -0.75$ and for various values of the reduced temperature.

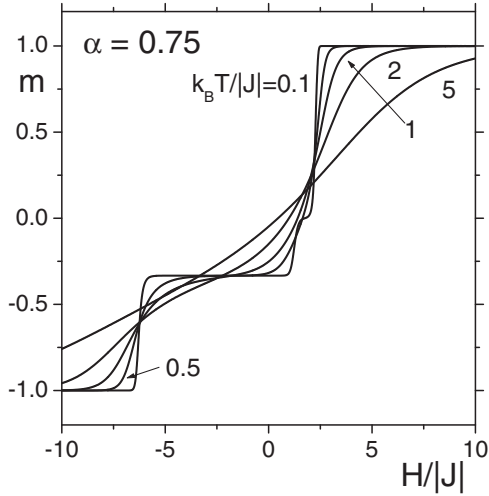


FIG. 6. The total magnetization per site as a function of the external magnetic field for $\alpha = 0.75$ and for various values of the reduced temperature.

value of α . Namely, for negative values of α , i.e., for α from the interval $-1 < \alpha < -0.5$, magnetization plateaus with $m = 0$ and $m = 1/3$ emerge for low enough temperatures, which are realized in the intervals $-3 - \alpha < H/|J| < 1 + 3\alpha$ and $1 + 3\alpha < H/|J| < 4 - 3\alpha$, respectively. Thus, it is evident that while the length of the magnetization plateau with $m = 1/3$ increases when the absolute value of α increases, the length of the plateau with $m = 0$ decreases and it disappears completely for $\alpha = -1$. On the other hand, for positive values of α , i.e., for α from the interval $0.5 < H/|J| < 1$, the situation is again opposite. Here, magnetization plateaus with $m = 0$ and $m = -1/3$ emerge when the temperature tends to zero and are realized in the intervals $-1 + 3\alpha < H/|J| < 3 - \alpha$ and $-4 - 3\alpha < H/|J| < -1 + 3\alpha$, respectively. The length of the magnetization plateau with $m = 1/3$ increases when the value of α increases and the length of the plateau with $m = 0$ again decreases and it disappears completely for $\alpha = 1$.

The last qualitatively different type of behavior of the magnetization is obtained for $|\alpha| > 1$. As it is evident from Figs. 7 and 8, where the total magnetization as a function of the external magnetic field for various values of the temperature is shown for $\alpha = -1.5$ (Fig. 7) and $\alpha = 1.5$ (Fig. 8), in this interval of absolute values of α only one magnetization plateau exists when the temperature tends to zero. Here, the magnetization plateau with $m = 1/3$ exists for $\alpha < -1$ and is realized in the interval $-2 < H/|J| < 4 - 3\alpha$. On the other hand, for $\alpha > 1$, the plateau with $m = -1/3$ emerges for low temperatures and is realized in the interval $-4 - 3\alpha < H/|J| < 2$.

Let us also briefly discuss the behavior of the total magnetization per site as a function of the reduced temperature in various regimes which are given by the typical values of the parameter α for various values of the external magnetic field. First of all, it is important to realize that there exists a simple relation between the values of the magnetization for positive and negative values of α , namely,

$$m\left(\frac{k_B T}{|J|}, \frac{H}{|J|}, \alpha\right) = -m\left(\frac{k_B T}{|J|}, -\frac{H}{|J|}, -\alpha\right). \quad (24)$$

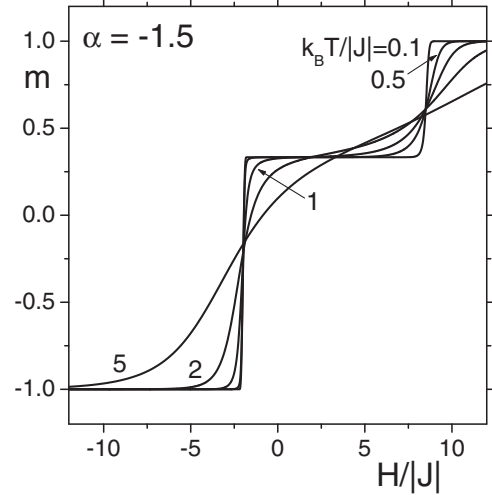


FIG. 7. The total magnetization per site as a function of the external magnetic field for $\alpha = -1.5$ and for various values of the reduced temperature.

The validity of this relation can be also verified in the pairs of Figs. 3 and 4, 5 and 6, and 7 and 8. Bearing in mind Eq. (24), it is sufficient to restrict our discussion to the positive values of α . Thus, in Figs. 9–11 three qualitatively different behaviors of the total magnetization per site are shown as functions of the reduced temperature for typical values of α , namely, for $\alpha = 0.25$ (Fig. 9), for $\alpha = 0.75$ (Fig. 10), and for $\alpha = 1.5$ (Fig. 11), as well as for various values of the external magnetic field. It is again evident that in the limit $T \rightarrow 0$ for a given value of α the magnetization can acquire only a few possible values which correspond to the possible ground states of the model. The number of possible ground states as well as the corresponding values of the magnetization depend on the value of α , namely, whether $|\alpha| < 0.5$, $0.5 < |\alpha| < 1$, or $|\alpha| > 1$. From Fig. 9 it is easy to see that for $|\alpha| < 0.5$ there exist nine different ground states. Two of them are the

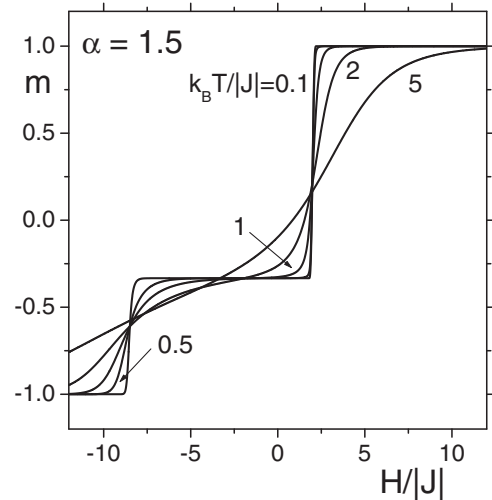


FIG. 8. The total magnetization per site as a function of the external magnetic field for $\alpha = -1.5$ and for various values of the reduced temperature.

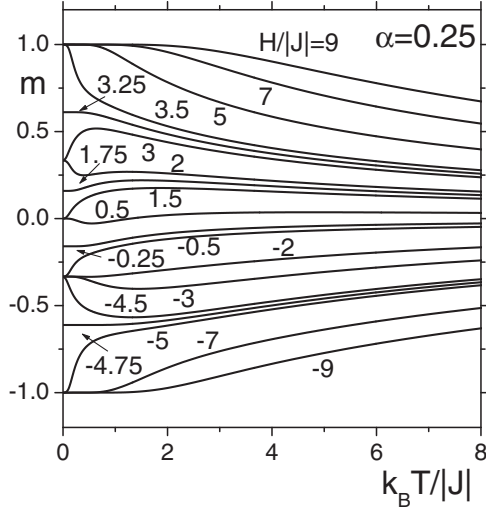


FIG. 9. The total magnetization per site as a function of the reduced temperature for $\alpha = 0.25$ as well as for various values of the external magnetic field $H/|J|$.

trivial saturated ground states with $m = \pm 1$ and three of them correspond to the nontrivial long-range-order ground states (plateaus) with the values of magnetization $m = 0$ and $m = \pm 1/3$ (see also Figs. 2, 3, and 4). In addition, there exist four other ground states which are realized only for exactly defined values of the external magnetic field (the corresponding values of the external field depend on the value of α) on the borders between various long-range-order ground states and are called the singular ground states (we shall discuss their properties in detail later).

On the other hand, as it follows from Fig. 10, there exist seven different ground states for $0.5 < |\alpha| < 1$. Two of them are again trivial saturated ground states with $m = \pm 1$. At the same time, there exist two nontrivial ground states in the form of plateaus with $m = 0$ and $m = 1/3$ for $-1 < \alpha < -0.5$ or

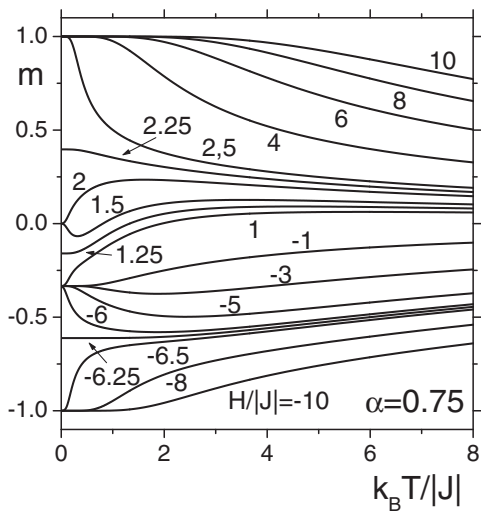


FIG. 10. The total magnetization per site as a function of the reduced temperature for $\alpha = 0.75$ as well as for various values of the external magnetic field $H/|J|$.

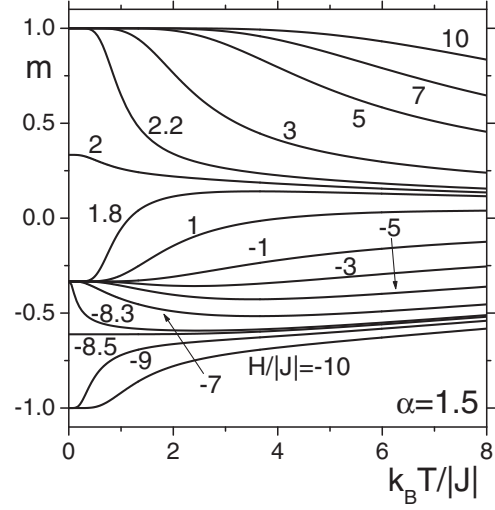


FIG. 11. The total magnetization per site as a function of the reduced temperature for $\alpha = 1.5$ as well as for various values of the external magnetic field $H/|J|$.

with $m = 0$ and $m = -1/3$ for $0.5 < \alpha < 1$. The last three ground states are again realized only for exactly defined values of the external magnetic field (the singular ground states) and represent intermediate states between various long-range-order ground states. Again, we shall discuss their properties a little bit later.

In the end, in the case of $|\alpha| > 1$ the model exhibits the existence of only five ground states in the limit $T \rightarrow 0$ (see Fig. 11). As is standard, two of them represent saturated ground states with $m = \pm 1$. In this case, however, there exists a single nontrivial long-range-order ground state with $m = 1/3$ for $\alpha < -1$ or with $m = -1/3$ for $\alpha > 0$. The remaining two ground states are the singular ground states which represent intermediate states between the only nontrivial plateau ground state and both saturated ground states and which are realized for exactly defined values of the external magnetic field.

In addition, however, specific situations come into being for border values of the parameter α , i.e., for $|\alpha| = 0.5$ as well as for $|\alpha| = 1$, when the absolute values of the multisite interaction are half of or equal to the nearest-neighbor antiferromagnetic interaction. For these special cases, the behavior of the magnetization as a function of the reduced temperature is shown in Figs. 12 and 13, respectively. Although, at first sight it seems that the behavior of the magnetization is similar to the corresponding behavior shown in Figs. 10 and 11, respectively, nevertheless, here qualitatively new singular ground states appear for exactly defined values of the external magnetic field (exact values of their magnetization will be found below). Namely, in the case $|\alpha| = 0.5$, these new singular ground states emerge for $H/|J| = -2.5$ and $\alpha = -0.5$ and for $H/|J| = 2.5$ and $\alpha = 0.5$. On the other hand, in the case $|\alpha| = 1$, new singular ground states appear for $H/|J| = -2$ and $\alpha = -1$ and for $H/|J| = 2$ and $\alpha = 1$.

B. The ground states of the model

Having the explicit expression for the total magnetization per site [see Eq. (23)] it is also possible to perform a completely

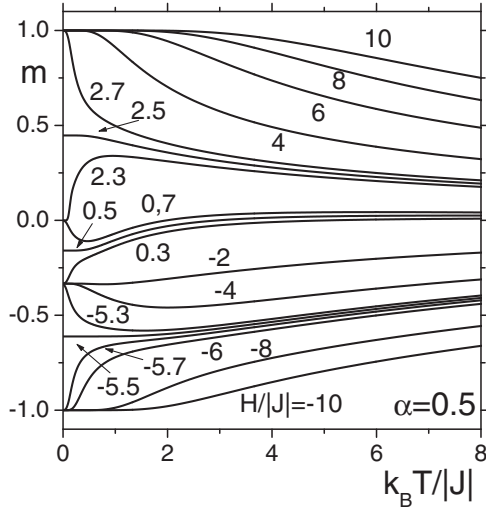


FIG. 12. The total magnetization per site as a function of the reduced temperature for $\alpha = 0.5$ as well as for various values of the external magnetic field $H/|J|$.

exact analysis of the properties of all ground states of the model, i.e., the structure of the total magnetization per site at $T = 0$. All ground states of the model are shown in Fig. 14 in the plane $H/|J|$ versus α . From Fig. 14 it is immediately evident that the whole plane $H/|J|$ - α is divided into five disjoint regions in which the plateaulike ground states with the values of the magnetization $m = 0$, $m = \pm 1/3$, and $m = \pm 1$ are realized. These regions are separated by lines at which various nontrivial singular ground states are obtained. In addition, at points at which three regions meet (or in which three different border lines join) additional nontrivial singular ground states appear. Let us discuss the properties of all singular ground states in some more detail.

The transitions between the saturated ground state with $m = -1$ and the plateau with $m = -1/3$ (the left solid line

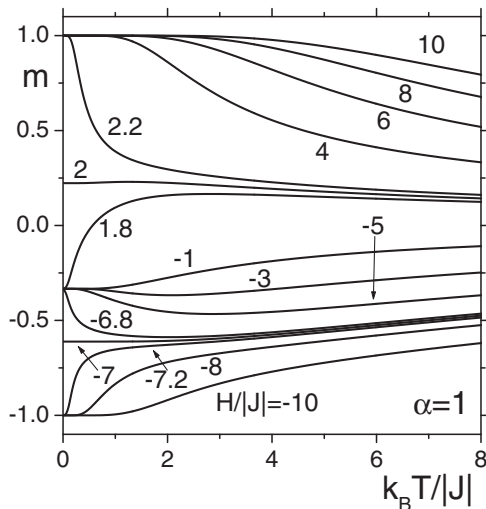


FIG. 13. The total magnetization per site as a function of the reduced temperature for $\alpha = 1$ as well as for various values of the external magnetic field $H/|J|$.

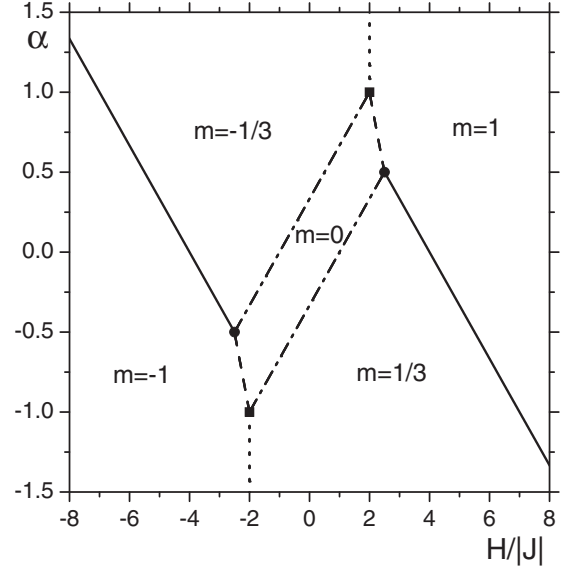


FIG. 14. The properties of the ground states of the model. The solid lines denote the positions of the singular ground states with total magnetization $m \approx -0.6115$ (left solid line) and $m \approx 0.6115$ (right solid line), the dashed lines denote positions of the singular ground states with $m \approx -0.3967$ (left dashed line) and $m \approx 0.3967$ (right dashed line), the dash-dotted lines correspond to the singular ground states with $m \approx -0.1593$ [left (upper) dash-dotted line] and $m \approx 0.1593$ [right (lower) dash-dotted line], and the dotted lines describe the singular ground states with $m = -1/3$ (left dotted line) and $m = 1/3$ (right dotted line). The two filled circles determine the positions of the singular ground states with $m \approx -0.4472$ (left filled circle) and $m \approx 0.4472$ (right filled circle) and the two filled squares show the positions of the singular ground states with $m \approx -0.2230$ (left filled square) and $m \approx 0.2230$ (right filled square).

in Fig. 14) as well as between the saturated ground state with $m = 1$ and the plateau with $m = 1/3$ (the right solid line in Fig. 14) are realized through the singular ground states with the following exact values of the magnetization:

$$m = \mp \frac{93 c_1^{1/3} (1 + 2\sqrt{d_1})^2 - 2^{5/3} \sqrt{93} (c_1^{2/3} - 2^{2/3})}{372 c_1^{1/3} \sqrt{d_1} (1 + 2\sqrt{d_1})}, \quad (25)$$

where

$$d_1 = \frac{1}{3} \left[\frac{19}{4} + \left(\frac{c_1}{2} \right)^{-1/3} + \left(\frac{c_1}{2} \right)^{1/3} \right], \quad (26)$$

$$c_1 = 29 + 3\sqrt{93}. \quad (27)$$

Their approximate numerical values are $m \approx \mp 0.611492$. The negative value of this magnetization is obtained on the border between long-range-order ground states with $m = -1$ and $m = -1/3$ (the left solid line in Fig. 14) defined by the the following relation:

$$\alpha = -\frac{1}{3} \left(\frac{H}{|J|} + 4 \right), \quad \frac{H}{|J|} < -2.5. \quad (28)$$

On the other hand, a positive value of the magnetization is realized on the border between the regions of the ground states with $m = 1$ and $m = 1/3$ (the right solid line in Fig. 14). This

border is given by the equation

$$\alpha = \frac{1}{3} \left(-\frac{H}{|J|} + 4 \right), \quad \frac{H}{|J|} > 2.5. \quad (29)$$

Further, the transitions between the saturated ground states with $m = \mp 1$ and the plateau with $m = 0$ (the dashed lines in Fig. 14) are realized through the singular ground states with the following exact values of magnetization:

$$m = \mp \frac{9e_1 + 8d_2^{3/2}(3 + e_1 + 2e_2) + 4d_2(11 - 2e_1e_2)}{16d_2^{3/2}e_2[1 + 2(e_2 + \sqrt{d_2})]}, \quad (30)$$

where

$$e_1 = 2d_3 + d_4 - \frac{25}{6}, \quad (31)$$

$$e_2 = \sqrt{\frac{19}{4} + \frac{9}{4\sqrt{d_2}}} - d_2, \quad (32)$$

$$d_2 = \frac{1}{3} \left[\frac{19}{4} + 16(-1)^{2/3} \left(\frac{c_2}{2} \right)^{-1/3} - \left(-\frac{c_2}{2} \right)^{1/3} \right], \quad (33)$$

$$d_3 = \frac{1}{3} \left[\frac{19}{4} + 16(-1)^{2/3} \left(\frac{c_2}{2} \right)^{-1/3} + \left(-\frac{c_2}{2} \right)^{1/3} \right], \quad (34)$$

$$d_4 = \frac{2^{1/3}c_3}{3c_2^{2/3}} \left[(-2)^{1/3} + \frac{32(-1)^{2/3}}{c_2^{2/3}} \right], \quad (35)$$

and

$$c_2 = 155 - 3\sqrt{849}, \quad (36)$$

$$c_3 = -137 + 539\sqrt{\frac{3}{283}}. \quad (37)$$

Their approximate numerical values are $m \approx \mp 0.396\ 651$. The negative value of this magnetization is obtained on the border between plateaus with $m = -1$ and $m = 0$ (the left dashed line in Fig. 14) defined by the relation

$$\alpha = -\frac{H}{|J|} - 3, \quad -2.5 < \frac{H}{|J|} < -2. \quad (38)$$

At the same time, the positive value of the magnetization is realized on the border between the regions of the ground states with $m = 1$ and $m = 0$ (the right dashed line in Fig. 14). This border is given by equation

$$\alpha = -\frac{H}{|J|} + 3, \quad 2 < \frac{H}{|J|} < 2.5. \quad (39)$$

On the other hand, the transition between the saturated ground state with $m = -1$ and the plateau with $m = 1/3$ [the left (lower) dotted line in Fig. 14 defined by the conditions $H/|J| = -2$ and $\alpha < -1$] as well as between the saturated ground state with $m = 1$ and the plateau with $m = -1/3$ [the right (upper) dotted line in Fig. 14 defined by conditions $H/|J| = 2$ and $\alpha > 1$] are realized through the singular ground states with the values of magnetization $m = -1/3$ and $m = 1/3$, respectively.

The last singular ground states which are realized on line segments are those which separate the plateau with $m = 0$ from

the plateaus with $m = \mp 1/3$ (they are denoted by the dash-dotted lines in Fig. 14). Their exact values of magnetization are

$$m = \mp \frac{d_5(4 + e_3e_4) - e_3(1 + d_5^{3/2})}{4d_5^{3/2}e_4(e_4 + \sqrt{d_5})}, \quad (40)$$

where

$$e_3 = 2d_6 + d_7 - \frac{8}{3}, \quad (41)$$

$$e_4 = \sqrt{4 + \frac{2}{\sqrt{d_5}}} - d_5, \quad (42)$$

$$d_5 = \frac{1}{3} \left[4 + 16(-1)^{2/3} \left(\frac{c_2}{2} \right)^{-1/3} - \left(-\frac{c_2}{2} \right)^{1/3} \right], \quad (43)$$

$$d_6 = \frac{1}{3} \left[4 + 16(-1)^{2/3} \left(\frac{c_2}{2} \right)^{-1/3} + \left(-\frac{c_2}{2} \right)^{1/3} \right], \quad (44)$$

$$d_7 = \frac{2^{1/3}c_4}{3c_2^{2/3}} \left[(-2)^{1/3} + \frac{32(-1)^{2/3}}{c_2^{2/3}} \right], \quad (45)$$

$$c_4 = -173 + 1159\sqrt{\frac{3}{283}}, \quad (46)$$

and c_2 is given in Eq. (36). Their approximate numerical values are $m \approx \mp 0.159\ 320$. The negative value of this magnetization is obtained on the border between plateaus with $m = -1/3$ and $m = 0$ [the left (upper) dash-dotted line in Fig. 14] given by the relation

$$\alpha = \frac{1}{3} \left(\frac{H}{|J|} + 1 \right), \quad -2.5 < \frac{H}{|J|} < 2. \quad (47)$$

At the same time, the positive value of the magnetization is realized on the border between plateaus with $m = 1/3$ and $m = 0$ [the right (lower) dash-dotted line in Fig. 14]. This border is given as follows:

$$\alpha = \frac{1}{3} \left(\frac{H}{|J|} - 1 \right), \quad -2 < \frac{H}{|J|} < 2.5. \quad (48)$$

As was already mentioned, there exist four other singular ground states with nontrivial values of the total magnetization per site which are realized at discrete points in the plane $H/|J| - \alpha$ at which three different regions of the corresponding long-range-order ground states meet. In Fig. 14, they are denoted by filled circles and squares. As it is evident from Fig. 14, two of these special ground states emerge at the point at which the plateaus with values of magnetization $m = -1$, $m = -1/3$, and $m = 0$ meet, i.e., at the point with coordinates $H/|J| = -2.5$ and $\alpha = -0.5$, as well as at the point at which the plateaus with values of magnetization $m = 1$, $m = 1/3$, and $m = 0$ meet, i.e., at the point with coordinates $H/|J| = 2.5$ and $\alpha = 0.5$. At these points the total magnetization per site obtains the following values:

$$m = \mp \frac{5 + 3\sqrt{5}}{5(3 + \sqrt{5})}. \quad (49)$$

Their approximate numerical values are $m \approx \mp 0.447\ 214$. The negative value of the magnetization is obtained for $H/|J| = -2.5$ and $\alpha = -0.5$ and the positive value for

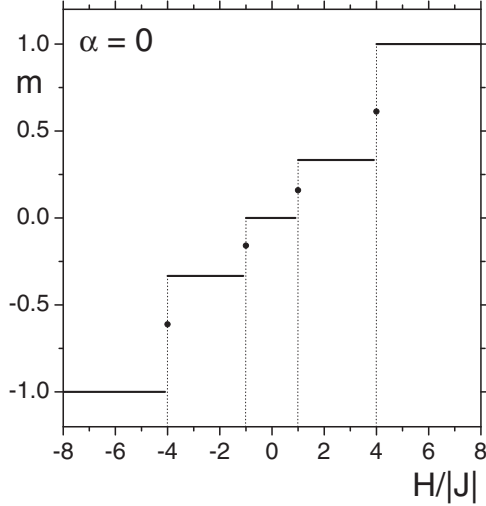


FIG. 15. The magnetization of the model as a function of the external magnetic field for $T = 0$ and $\alpha = 0$. The singular ground states at $H/|J| = \mp 4$ have the values of magnetization $m \approx \mp 0.611492$ and the singular ground states at $H/|J| = \mp 1$ have the values of magnetization $m \approx \mp 0.159320$.

$H/|J| = 2.5$ and $\alpha = 0.5$. In Fig. 14, they are denoted by filled circles.

Finally, the second and, at the same time, the last couple of singular ground states, which are realized at discrete points in the plane $H/|J| - \alpha$ and which are denoted by filled squares in Fig. 14, emerge at the point at which the plateaus with values of magnetization $m = -1$, $m = 0$, and $m = 1/3$ meet, i.e., at the point with coordinates $H/|J| = -2$ and $\alpha = -1$, as well as at the point at which the plateaus with values of magnetization $m = 1$, $m = 0$, and $m = -1/3$ meet, i.e., at the point with coordinates $H/|J| = 2$ and $\alpha = 1$. At these points the total magnetization per site obtains the values

$$m = \mp \frac{62c_5^{4/3} - (2c_5)^{2/3}c_6 + 2^{4/3}c_7}{62c_5^{4/3} \left[1 + 7\left(\frac{c_5}{2}\right)^{-1/3} + \left(\frac{c_5}{2}\right)^{1/3} \right]}, \quad (50)$$

where

$$c_5 = 47 + 3\sqrt{93}, \quad (51)$$

$$c_6 = 31 + 27\sqrt{93}, \quad (52)$$

$$c_7 = 3131 + 375\sqrt{93}. \quad (53)$$

Their approximate numerical values are $m \approx \mp 0.222984$. The negative value of the magnetization is obtained for $H/|J| = -2$ and $\alpha = -1$ and the positive value for $H/|J| = 2$ and $\alpha = 1$ (see Fig. 14).

The existence of the various types of singular ground states discussed above means that all transitions between different long-range-order ground states (saturated ground states and various plateaus) are realized through intermediate ground states with nontrivial values of the total magnetization per site, as is demonstrated explicitly in Fig. 15 for the special case with $\alpha = 0$. Using the phase diagram of all ground states (Fig. 14) analogous figures can be immediately drawn for arbitrary values of α . Thus, we can conclude that the properties of all ground states of the present model are completely known now.

Without doubt the very existence as well as the rather complicated structure of the nontrivial singular ground states are some of the most important and intriguing results of the present paper. Recently, the existence of the singular ground states was also exactly proven in the framework of the antiferromagnetic Ising model on the simplest pure Husimi lattice built up from elementary triangles and with the coordination number $z = 4$, which represents an approximation of the model on the regular two-dimensional kagome lattice [7,8], as well as in the framework of the antiferromagnetic Ising model on the tetrahedron recursive lattice [9]. Nevertheless, in principle, the complicated structure of the singular ground states in these models can always be considered as an effect of the recursive form of the lattices. However, as shown in the present paper, the nontrivial structure of the singular ground states also exists in the framework of the antiferromagnetic Ising model on a well-defined regular lattice, namely, on the one-dimensional zigzag ladder lattice. In our opinion, this is a nontrivial fact which must also be taken into account when various classical antiferromagnetic models are considered on regular two- or three-dimensional geometrically frustrated lattices such as the kagome lattice, the triangular lattice, or the tetrahedron (pyrochlore) lattice.

However, it is also worth mentioning that the exact properties of the singular ground states, e.g., such as those given in the present paper, can be studied only in the framework of exactly solvable models, where properties of the magnetization can be analyzed in the limit $T \rightarrow 0$. Therefore, we are afraid that the properties of the singular ground states in various antiferromagnetic models on frustrated regular two- and three-dimensional lattices cannot be obtained (at least for now) simply because there do not exist exact solutions of these models in a nonzero external magnetic field. On the other hand, the exact properties of the ground states in these models can hardly be found by using approximative or pure numerical methods.

The fact that the magnetization between various plateaulike ground states behaves discontinuously lures one to consider these transitions as first-order phase transitions. However, we do not think that this is correct, simply because even the principal condition for the existence of a first-order phase transition is not fulfilled here, namely, there is no coexistence of the phases at these points. Strictly speaking, in our model only one phase exists for all values of the parameters of the model, which is defined by the eigenvalue λ_1 given in Eq. (11). The magnetization related to this single phase is a continuous function for arbitrary $T > 0$, and for $T = 0$ it becomes a discontinuous function which decays into disjoint plateaulike ground states and singular ground states. But it is necessary to bear in mind that we are still working in the framework of the same phase, i.e., all the ground states are defined by the same solution (phase) of the model. Therefore, we think that we are facing a different phenomenon here which cannot be simply included and described in the framework of first-order phase transitions.

C. The entropy and the degeneracy of the ground states

Having the exact expression for the free energy per site of the present model given in Eq. (10) the macroscopic degeneracy of the ground states can be studied by calculation of the

entropy. The macroscopic degeneracy Ω is related to the entropy S of the entire system through the well-known relation given in the framework of the microcanonical ensemble, namely,

$$S = k_B \ln \Omega. \quad (54)$$

On the other hand, the entire entropy of the present model on a lattice which consists of N sites is given as follows:

$$S \equiv -N \frac{\partial f}{\partial T} = \frac{k_B N}{2} \left(\ln \lambda_1 + \frac{T}{\lambda_1} \frac{\partial \lambda_1}{\partial T} \right), \quad (55)$$

where we have used the explicit expression for the free energy per site given in Eq. (10). By performing the corresponding calculations one can easily write out the explicit expression for the entropy. Therefore, it is not necessary to present its explicit form here. Instead let us discuss briefly the properties of the entropy of all ground states of the model. At the same time, by comparison of the expressions for the entropy given in Eqs. (54) and (55) the macroscopic degeneracies of the ground states can be immediately found.

First of all, as expected, the entropy of all plateaulike ground states with values of magnetization $m = 0$, $\pm 1/3$, and ± 1 is zero, i.e., all of them have finite degeneracies which can be easily determined. However, the finite degeneracies also exist for all the singular ground states which lie on dotted lines in Fig. 14 with the values of magnetization $m = \pm 1/3$, i.e., the entropy of these singular ground states is also equal to zero. This means that the direct transitions between the plateau ground state with $m = -1/3$ and the saturated ground state with $m = 1$, which is realized through the singular ground state with $m = 1/3$, as well as between the plateau ground state with $m = 1/3$ and the saturated ground state with $m = -1$, which is realized through the singular ground state with $m = -1/3$, are not accompanied by a discontinuity of the entropy.

On the other hand, all the other transitions between various plateaus are always accompanied by discontinuity of the entropy, i.e., the corresponding singular ground states have infinite macroscopic degeneracies. The corresponding entropies are the following: the entropy of the singular ground states with $m \approx \pm 0.6115$ (solid lines in Fig. 14) is $S \approx 0.3822Nk_B$, the entropy of the singular ground states with $m \approx \pm 0.3967$ (dashed lines in Fig. 14) is $S \approx 0.3223Nk_B$, the entropy of the singular ground states with $m \approx \pm 0.1593$ (dash-dotted lines in Fig. 14) is $S \approx 0.1995Nk_B$, the entropy of the singular ground states with $m \approx \pm 0.4472$ (filled circles in Fig. 14) is $S \approx 0.4812Nk_B$, and the entropy of the singular ground states with $m \approx \pm 0.2230$ (filled squares in Fig. 14) is $S \approx 0.3822Nk_B$. Here, it is also interesting that two completely different singular ground states with $|m| \approx 0.6115$ and with $|m| \approx 0.2230$ have the same value of the entropy. It also means that they have the same value of the macroscopic degeneracy.

V. CONCLUSION

In conclusion, in this paper we have investigated the antiferromagnetic spin-1/2 Ising model with multisite interaction in the presence of an external magnetic field on the infinite triangular zigzag ladder, which represents the

simplest geometrically frustrated system. First of all, it is shown that the model is exactly analytically solvable and the exact solution of the model is found by using the transfer matrix method.

Further, by using the exact expression for the total magnetization per site of the model, the properties of the magnetization as a function of the temperature, as a function of the external magnetic field, and as a function of the parameter which describes the presence of the multisite interaction are investigated in detail (see Figs. 2–13). It is shown that for low values of temperature, i.e., for $k_B T/|J| \ll 1$, magnetization plateaus with $m = \pm 1/3$ and $m = 0$ appear as a consequence of the frustration. At the same time, however, it is also shown that the behavior of the magnetization strongly depends on the ratio $\alpha = J'/|J|$, i.e., on the strength of the multisite interaction compared with the antiferromagnetic nearest-neighbor interaction. In this respect, all three above-mentioned plateaus at low temperatures exist only for $|\alpha| < 0.5$ and their lengths depend on the value of α . On the other hand, for $0.5 < |\alpha| < 1$ only two plateaus are realized, namely, the plateaus with $m = 0$ and $m = -1/3$ for positive values of α and the plateaus with $m = 0$ and $m = 1/3$ for negative values of α . Finally, only one plateau emerges at low temperatures for $|\alpha| > 1$, namely, the plateau with $m = -1/3$ for $\alpha > 1$ and the plateau with $m = 1/3$ for $\alpha < -1$.

In addition, having the exact expression (23) for the total magnetization per site we have also performed an exact analysis of the properties of all possible ground states of the model. It is shown that besides the plateaulike ground states, i.e., the saturated ground states with $m = \pm 1$ and the above-mentioned plateaus with $m = \pm 1/3$ and $m = 0$, there also exists a nontrivial set of so-called singular ground states which are realized on the line segments which correspond to the borders between various regions in which the long-range-order ground states exist. It is also shown that at points at which three of these regions meet still other nontrivial singular ground states emerge. The exact values of the magnetization as well as their coordinates in the plane $H/|J|$ versus α are found for all these singular ground states.

The exact analysis of the properties of the ground states with the existence of the singular ground states with nontrivial values of magnetization is one of the main results of the present paper. Another nontrivial conclusion of the paper is the very fact that all transitions between different plateaus as well as between plateaus and saturated ground states are always realized through the corresponding intermediate singular ground states, as was already seen earlier in the framework of the antiferromagnetic Ising models on geometrically frustrated recursive lattices (see Refs. [7–9]). Therefore, we suppose that the existence of the singular ground states is not a specific property of the present model but rather it is a general feature of all classical models of frustrated magnetic systems.

In addition, we have also investigated and discussed briefly the macroscopic degeneracy of all ground states of the model by analyzing the explicit expression for the entropy in the limit $T \rightarrow 0$. It is shown that although most of the singular ground states exhibit nonzero entropy, i.e., these ground states are infinitely degenerate, there also exist singular ground states with finite degeneracy, i.e., which have zero value of the entropy.

Thus, finally, we can conclude that the magnetization properties of the antiferromagnetic Ising model with multisite interaction on an infinite zigzag ladder are completely known now. We also suppose that the technique used in the present paper, which has allowed us to solve the model exactly, can be generalized and applied for investigation of more general antiferromagnetic Ising and Ising-like models on various zigzag ladders. We believe that many interesting results can be obtained in this direction.

ACKNOWLEDGMENTS

The authors gratefully acknowledge the hospitality of the Bogoliubov Laboratory of Theoretical Physics of the Joint Institute for Nuclear Research, Dubna, Russian Federation. The work was supported by the VEGA Grant No. 2/0093/13 of the Slovak Academy of Sciences and by the realization of the Project ITMS No. 26220120009, based on the Supporting Operational Research and Development Program financed from the European Regional Development Fund.

-
- [1] J. E. Greedan, *J. Mater. Chem.* **11**, 37 (2001).
 [2] G. Toulouse, *Commun. Phys.* **2**, 115 (1977).
 [3] H. T. Diep, M. Debauche, and H. Giacomini, *Phys. Rev. B* **43**, 8759 (1991).
 [4] *Frustrated Spin Systems*, edited by H. T. Diep (World Scientific, Singapore, 2004).
 [5] R. J. Baxter, *Exactly Solved Models in Statistical Mechanics* (Academic Press, London, 1982).
 [6] G. H. Wannier, *Phys. Rev.* **79**, 357 (1950).
 [7] E. Jurčišinová, M. Jurčišin, and A. Bobák, *Phys. Lett. A* **377**, 2712 (2013).
 [8] E. Jurčišinová, M. Jurčišin, and A. Bobák, *J. Stat. Phys.* **154**, 1096 (2014).
 [9] E. Jurčišinová and M. Jurčišin, *Phys. Rev. E* **89**, 032123 (2014).
 [10] M. Matsuda and K. Katsumata, *J. Magn. Magn. Mater.* **140**, 1671 (1995).
 [11] M. Matsuda *et al.*, *Phys. Rev. B* **55**, R11953 (1997).
 [12] M. Azuma, Z. Hiroi, M. Takano, K. Ishida, and Y. Kitaoka, *Phys. Rev. Lett.* **73**, 3463 (1994).
 [13] T. Imai, K. R. Thurber, K. M. Shen, A. W. Hunt, and F. C. Chou, *Phys. Rev. Lett.* **81**, 220 (1998).
 [14] Y. Mizuno, T. Tohyama, S. Maekawa, T. Osafune, N. Motoyama, H. Eisaki, and S. Uchida, *Phys. Rev. B* **57**, 5326 (1998).
 [15] G. Chaboussant, P. A. Crowell, L. P. Lévy, O. Piovesana, A. Madouri, and D. Maillé, *Phys. Rev. B* **55**, 3046 (1997).
 [16] W. Shiramura, K. Takatsu, H. Tanaka, K. Kamishina, M. Takahashi, H. Mitamura, and T. Goto, *J. Phys. Soc. Jpn.* **66**, 1900 (1997).
 [17] W. Shiramura *et al.*, *J. Phys. Soc. Jpn.* **67**, 1548 (1998).
 [18] S.-L. Drechsler, N. Tristan, R. Klingeler, B. Büchner, J. Richter, J. Malek, O. Volkova, A. Vasiliev, M. Schmitt, A. Ormeci, C. Loison, W. Schnelle, and H. Rosner, *J. Phys.: Condens. Matter* **19**, 145230 (2007).
 [19] Z. N. C. Ha, *Phys. Rev. B* **59**, 1559 (1999).
 [20] N. Maeshima and K. Okunishi, *Phys. Rev. B* **62**, 934 (2000).
 [21] K. Okunishi and N. Maeshima, *Phys. Rev. B* **64**, 212406 (2001).
 [22] J. Schulenburg, A. Honecker, J. Schnack, J. Richter, and H.-J. Schmidt, *Phys. Rev. Lett.* **88**, 167207 (2002).
 [23] I. Bose and E. Chattopadhyay, *Phys. Rev. A* **66**, 062320 (2002).
 [24] M. T. Batchelor, X.-W. Guan, N. Oelkers, K. Sakai, Z. Tsuboi, and A. Foerster, *Phys. Rev. Lett.* **91**, 217202 (2003).
 [25] H. T. Lu, Y. J. Wang, Shaojin Qin, and T. Xiang, *Phys. Rev. B* **74**, 134425 (2006).
 [26] D. V. Dmitriev and V. Ya. Krivnov, *Phys. Rev. B* **77**, 024401 (2008).
 [27] D. N. Sheng, O. I. Motrunich, and M. P. A. Fisher, *Phys. Rev. B* **79**, 205112 (2009).
 [28] T. Hikihara, T. Momoi, A. Furusaki, and H. Kawamura, *Phys. Rev. B* **81**, 224433 (2010).
 [29] S. Furukawa, M. Sato, S. Onoda, and A. Furusaki, *Phys. Rev. B* **86**, 094417 (2012).
 [30] I. T. Shyiko, I. P. McCulloch, J. V. Gumenjuk-Sichevska, and A. K. Kolezhuk, *Phys. Rev. B* **88**, 014403 (2013).
 [31] F. A. Kassan-ongly, *Phase Transitions* **74**, 353 (2001).
 [32] V. V. Hovhannisyan and N. S. Ananikian, *Phys. Lett. A* **372**, 3363 (2008).
 [33] Yu. I. Dublenych, *J. Phys.: Condens. Matter* **25**, 406003 (2013).
 [34] J. Strečka, O. Rojas, T. Verkholyak, and M. L. Lyra, *Phys. Rev. E* **89**, 022143 (2014).